УДК 551.465

© *Г. Вяли*[1], *В. М. Журбас*[2*]

[1]Таллиннский технологический университет, Кафедра морских систем, 12618, Академиа тээ, 15А, г. Таллинн, Эстония
[2]Институт океанологии им. П.П. Ширшова РАН, 117997, Нахимовский пр., д. 36, г. Москва, Россия
*E-mail: zhurbas@ocean.ru

СЕЗОННОСТЬ СУБМЕЗОМАСШТАБНЫХ КОГЕРЕНТНЫХ ВИХРЕЙ В СЕВЕРНОЙ БАЛТИКЕ: МОДЕЛЬНОЕ ИССЛЕДОВАНИЕ

Статья поступила в редакцию 29.03.2021, после доработки 25.06.2021

Моделирование северной части собственно Балтийского моря с очень высоким разрешением показывает, что летом образуются циклонические и антициклонические субмезомасштабные когерентные вихри (СКВ) с экстремумом вертикальной завихренности в поверхностном слое, в то время как подповерхностные антициклонические СКВ в форме выпуклых линз в поле плотности преобладают над циклоническими СКВ – вогнутыми линзами с экстремумом вертикальной завихренности в холодном промежуточном слое ниже сезонного термоклина и выше перманентного галоклина. Зимой сезонный термоклин и холодный промежуточный слой сменяются относительно глубоким конвективно-перемешанным слоем, что делает невозможным образование подповерхностных вогнутых циклонических и выпуклых антициклонических линз. Вместо этого преобладают зимние циклонические СКВ с экстремальной вертикальной завихренностью на поверхности. Ядро зимних циклонических СКВ характеризуется отрицательной температурной аномалией во всем конвективно-перемешанном слое. В течение своего жизненного цикла длительностью до нескольких месяцев и более, смоделированный СКВ может многократно сливаться с другими СКВ того же знака завихренности, и слияние делает вихрь сильнее, тем самым способствуя его долговечности.

Ключевые слова: Балтийское море, численное моделирование с очень высоким разрешением, субмезомасштабный когерентный вихрь, гравитационная конвекция во вращающейся жидкости.

© *G. Väli*[1], *V. M. Zhurbas*[2*]

[1]Tallinn University of Technology, Department of Marine Systems, 12618, Akadeemia tee, 15A, Tallinn, Estonia
[2]Shirshov Institute of Oceanology, RAS, 117997, Nahimovsky Pr., 36, Moscow, Russia
*E-mail: zhurbas@ocean.ru

SEASONALITY OF SUBMESOSCALE COHERENT VORTICES IN THE NORTHERN BALTIC PROPER: A MODEL STUDY

Received 29.03.2021, in final form 25.06.2021

A very high-resolution modelling of the northern Baltic Proper shows that in summer the cyclonic and anticyclonic submesoscale coherent vortices (SCVs) with the extremum of vertical vorticity in the surface layer are formed, while the subsurface anticyclonic SCVs in the shape of convex lenses in the density field prevail over the cyclonic SCVs – concave lenses, with the vertical vorticity extremum in the cold intermediate layer below the seasonal thermocline and above the permanent halocline. In winter the seasonal thermocline and cold intermediate layer are replaced by a relatively deep convectively-mixed layer which makes the formation of subsurface concave cyclonic and convex anticyclonic lenses impossible there. Instead, the winter-time cyclonic SCVs with the vertical vorticity extremum at the surface dominate. The core of winter-time cyclonic SCVs is characterized by a negative temperature anomaly throughout the mixed layer. During its life cycle lasting up to several months and more, the modelled SCVs can repeatedly merge with other SCVs of the same sign of vorticity, and the merger makes the eddy stronger thereby contributing to its longevity.

Key words: Baltic Sea, very high-resolution numerical modelling, submesoscale coherent vortex, gravitational convection in rotating fluid.

Ссылка для цитирования: *Вяли Г.*, *Журбас В.М.* Сезонность субмезомасштабных когерентных вихрей в северной Балтике: модельное исследование // Фундаментальная и прикладная гидрофизика. 2021. Т. 14, № 3. С. 122—129. doi: 10.7868/S2073667321030114

For citation: *Väli G.*, *Zhurbas V.M.* Seasonality of Submesoscale Coherent Vortices in the Northern Baltic Proper: A Model Study. *Fundamentalnaya i Prikladnaya Gidrofizika*. 2021, 14, 3, 122—129. doi: 10.7868/S2073667321030114

1. Introduction

Submesoscale Coherent Vortices (SCVs) are defined as intense, long-living, rotary circulations which are approximately symmetric about vertical axes [1]. SCVs are abundant in the interior of the ocean, where their typical dimensions are 10 km horizontally and 100 m vertically, and the lifetimes can be as long as many years, during which entire ocean basins can be traversed [2]. A typical example of SCVs are Meddies, the anticyclonic, convex lenses of saltier and warmer water of the Mediterranean origin travelling in the main pycnocline of the North Atlantic [3, 4].

SCVs differ from classic mesoscale eddies whose horizontal dimension is determined by the first baroclinic deformation radius l_d, and which are characterized by a small Rossby number $\mathrm{Ro} = \zeta / f \ll 1$ and large Richardson number $\mathrm{Ri} = N^2 / \left(u_z^2 + v_z^2\right) \gg 1$, where $\zeta = -u_y + v_x$ is the vertical relative vorticity, f is the vertical planetary vorticity (Coriolis parameter), N is the buoyancy frequency, (u,v) are the horizontal components of flow velocity along x and y axes, the x, y and z subscripts denote the respective gradients/derivatives. The horizontal dimension of SCVs is usually smaller than l_d and determined by a local baroclinic radius of deformation Nh / f, where h is the vertical dimension of SCV. More importantly that SCVs are characterized by intermediate values of the Rossby and Richardson numbers of the order of unity: $\mathrm{Ro} = O(1)$, $\mathrm{Ri} = O(1)$ [5].

The dominance of anticyclonic SCVs over cyclonic ones throughout the ocean interior was originally explained by local diapycnal mixing events that create a stratification anomaly followed by geostrophic adjustment of the vortical flow [1, 2, 6]. A more refined interpretation is that SCVs usually form from separating, violently unstable boundary currents that induce strong mixing and roll up into vortices [5, 7]. High-resolution numerical modelling does reproduce spatially sparse, but ubiquitous SCVs in the surface layer of the ocean with noticeable asymmetry in vorticity: cyclonic vorticity is typically stronger due to finite-Ro effects of vortex stretching and inertial instability that limit the anticyclonic vorticity to $\zeta / f \gtrsim -1$, while the cyclonic vorticity can be as large as $\zeta / f > 2$ (e. g. [7, 8]).

Studies of SCVs in the Baltic Sea have a long history. Subsurface anticyclonic SCVs in the shape of convex lenses in the density field centered in the cold intermediate layer were recorded in the course of closely spaced CTD profiling and surveying in the East Gotland Basin in the eighties of the last century [9]. A cyclonic SCVs (a concave lens in the density field) was recorded within the permanent halocline south of the Gotland Deep after the Major Inflow 1993 [10]. Afterwards subsurface cyclonic SCVs – concave lenses were found in the Arkona Basin [11], Bornholm Basin [12], Słupsk Furrow and Gulf of Gdansk [13] and simulated in the framework of high-resolution circulation models [13—15]. Following Spall and Price [16], it was assumed that the subsurface cyclonic SCVs are formed due to the adjustment of the high potential vorticity inflow water column to a low potential vorticity environment [14]. High resolution images of the sea surface both provided by remote sensing and simulated within high-resolution circulation models show ubiquitous occurrence of cyclonic and anticyclonic SCVs in the upper layer including the surface mixed layer, the seasonal thermocline and partially the intermediate cold layer of the Baltic Sea [17—21]. Detection and tracking methods of SCVs in the Baltic Sea as applied to the field data of CTD profiling and the high-resolution modelling were developed in [22] and [23], respectively.

The Baltic Sea is characterized by a prominent seasonality of the thermohaline stratification. In summer, there are two pycnocline structure of water column with the upper mixed layer, the seasonal thermocline, the cold, low-stratified intermediate layer, and the permanent halocline typically occupying the depth ranges of 0—10 m, 10—30 m, 30—60 m, and > 60 m, respectively. In winter, the upper mixed layer, the seasonal thermocline, and the cold, low-stratified intermediate layer are replaced by a thick cold mixed layer formed due to gravitational convection caused by the cooling from the surface and enhanced wind forcing. Such drastic changes in vertical stratification inevitably imply strong seasonality of the SCVs, because neither the upper layer eddies whose baroclinicity is determined by deformations of the seasonal thermocline nor the subsurface rotating concave and convex lenses centered in the cold intermediate layer can exist in the winter season. The objective of this work is to investigate seasonality of the CSV characteristics in the Baltic Sea based on the results of high-resolution model simulations.

2. Model description

A detailed description of the model setup is done in [21], and here we briefly dwell on the main points.

The General Estuarine Transport Model (GETM) [24] is applied. GETM is a primitive equation, free surface, hydrostatic model with the embedded vertically adaptive coordinate scheme [25, 26]. The vertical mixing is parametrized by a k-e turbulence model coupled with an algebraic second-moment closure [27, 28].

The high-resolution nested model has a horizontally uniform step of 0.125 nautical miles (approximately 232 m) and 60 adaptive layers in vertical all over the computational domain covering the central Baltic Sea along with the Gulf of Finland and Gulf of Riga (Fig. 1, see Inset). The digital topography of the Baltic Sea with the resolution of 500 m

(approximately 0.25 nautical miles) was obtained from the Baltic Sea Bathymetry Database (http://data.bshc.pro/) and interpolated bilinearly to the model grid.

The nested model domain has the western open boundary in the Arkona Basin and the northern open boundary at the entrance to the Bothnian Sea (see Fig. 1). For the open boundary conditions the one-way nesting approach is used and the results from a coarse-resolution model with 0.5 nautical mile grid (926 m) are applied. The coarse resolution model run started from 01/04/2010 with initial thermohaline conditions taken from the Baltic Sea reanalysis for the 1989—2015 by the Copernicus Marine service. More detailed information on the coarse-resolution model is available in [29, 30].

The atmospheric forcing is taken from the High Resolution Limited Area Model (HIRLAM) maintained operationally by the Estonian Weather Service with the spatial resolution of 11 km [31].

The initial thermohaline field is obtained from the coarse-resolution model and interpolated horizontally to the high-resolution model domain. Information on the validation of the high-resolution and coarse-resolution models can be found in [21, 29].

Results of two runs of the nested model are analysed: a 7 months run and a year and a half run covering the period from 01.04.2018 to 31.10.2018 and from 01.04.2015 to 04.10.2016, respectively.

Before proceeding with the analysis of the simulation results, we note that the coarse-resolution model (926 m grid), whose output was used as the initial and open boundary conditions in the nested, high-resolution model (232 m grid), has been thoroughly tested by means of comparison of the simulated and observed current velocity variance and timeseries of sea-level fluctuations, temperature and salinity in the surface, intermediate and bottom layers for a number of monitoring stations of the Baltic Sea (see [29]). The ability of the nested, very high-resolution model to reproduce the observed SCVs is demonstrated in Fig. 2 (see Inset) where the satellite-born optical images of a $1^\circ \times 1^\circ = 111$ km $\times$ 111 km area of the northern Baltic Proper to the northeast of the Gotland Island from Sentinel-2 dated 2018-07-10 and 2018-07-15 are given versus the simulated maps of Ro in the surface layer for the same dates. The snapshots were taken during the period of summer blooming of cyanobacteria, when the submesocale motions have assembled the phytoplankton material into linear structures winded up into spirals thereby visualizing SCVs. Both the remote sensing images and simulated Ro maps display patterns densely populated with SCVs of a comparable length scale. Of course, one cannot expect that the model will reproduce the mutual arrangement of vortices in the remote sensing images, since it is impossible to simulate an individual realization of the random process of SCVs formation.

3. Results

To identify SCVs we will mostly stick to maps and vertical sections of the gradient Rossby number Ro calculated from the model output though the velocity differences at the horizontal step of 232 m. By painting the areas of positive and negative Ro values with red and blue of varying intensity, we expect to obtain on the map an image of cyclonic and anticyclonic eddies in the form of rounded spots of red and blue, respectively. The seasonality of SCVs is illustrated by simulation results related to warm season characterized by the presence of seasonal thermocline and cold intermediate layer, and cold season when there is a relatively deep convectively-mixed upper layer instead. We will conventionally call the warm season summer, and the cold season winter.

3.1. Summer season

The Ro maps shown in Fig. 3 (see Inset) displays a plenty of rounded blue and red spots in the surface layer ($z = 0$ m) with typical diameter of the order of 10 km which present anticyclonic and cyclonic eddies, respectively. Most of the eddies weaken with depth, but some of the anticyclonic ones intensify (see e. g. the blue spots located at approx. (19°E, 57°N) and (19.8°E, 58.1°N)) which are clearly seen on the $z = 60$ m level and not seen or almost not seen on the $z = 0$ m level).

Vertical structure of SCVs is illustrated in Fig. 4 (see Inset) where the Rossby number Ro, Richardson number Ri, potential density anomaly σ_θ, and temperature T versus distance and depth are presented for two crossing sections shown in Fig. 3. The surface-layer SCVs, which by definition are characterized by extreme values of Ro in the surface layer, have the shape of an inverted cone with the base of the cone on the surface (Fig. 4, *a*). Apart of the surface SCVs, several subsurface SCVs can be identified in Fig. 4, *c* which are characterized by extreme values of Ro in the interior, stratified layers and have the shape of concave and convex lenses for cyclones and anticyclones, respectively, in the density field. Most prominent, largest subsurface SCVs are located in the cold intermediate layer and immediately below it approximately at $z = 50$ m, while in the deeper salinity-stratified layer, the SCVs have smaller horizontal and vertical

size (Fig. 4, *c*). The cyclonic SCVs are characterized by faster rotation relative to the anticyclonic ones: in accordance to Fig. 4 the maximum value of Ro in the cyclonic SCVs varies within [1.20, 2.46] while the minimum value of Ro in the anticyclonic SCVs varies within [−0.91,−1.14]. Fig. 4 also displays the tendency for the Richardson number to decrease to $\mathrm{Ri} < 10$ at the periphery of SCVs which is typical for submesoscale dynamics [5].

A possible empirical scenario of formation of the surface-layer cyclonic SCVs is illustrated in Fig. 5 (see Inset) where a sequence of Ro snapshots west of the Gotland Island is presented. Northeasterly wind produces coastal upwelling along the western shore, and the related jet-like current and strip of cyclonic vorticity aligned to 0—40 m depth contours are formed which is probably caused by the stretching of vortex tubes in the course of upwelling. When the upwelling-favourable wind weaken, the strip of cyclonic vorticity becomes unstable and splits into a chain of four cyclonic eddies.

Similar descriptive scenario is applicable to the formation of subsurface anticyclonic lens pointed by an arrow in Figs. 3, 4, and 6. As shown in Fig. 6 (see Inset), the lens is initialized by a strip of high anticyclonic vorticity elongated along the 60-m isobaths. The strip is formed above the steepest bottom near the northeastern tip of the Gotland Island (see the 2018-05-16 07:12 snapshot). The anticyclonic vorticity strip, in its turn, is probably caused by squeezing of vortex tubes in the course of downwelling above the sloping bottom. Throughout its life cycle, the anticyclonic lens has twice merged with other anticyclonic lenses (first time on May 25—29, 2018 and second time on June 28—30, 2018, which led to its strengthening and long-term existence. The merging process can be qualitatively described as bringing the anticyclonic lenses closer to each other, involving them in anticyclonic rotation relative to the common center of mass, and eventual formation of a homogeneous rounded region of anticyclonic vorticity. The anticyclonic lens dissipated on September 26, 2018 entering a shallow bank southwest of the Saaremaa Island.

3.2. Winter season

Maps of Ro in winter season display a pattern of SCVs which is quite different from that of summer season (cf. Figs. 7—8 with Figs. 3, 5, and 6). On the levels $z = 0$, 40, and 60 m, which in winter relate to the convectively mixed upper layer, there is clear dominance of cyclonic eddies over anticyclonic ones. Actually, in the convectively mixed upper layer we observe only cyclonic SCVs whose diameter, including a core with high positive value of Ro and the surrounding ring where $\mathrm{Ro} \approx 0$, can reach up to 20—30 km. Instead of well-formed anticyclonic SCVs, we observe irregular rounded and elongated spots of high negative value of Ro with transverse horizontal lengthscale of the order of 1—2 km. In the deep layers that are not directly influenced by the atmospheric forcing, in winter the subsurface anticyclonic and less often cyclonic SCVs are more common – convex and concave density lenses of smaller size similar to those of summer season.

The side view of a winter-time cyclonic SCVs, which is pointed by the arrow in Figs. 7 and 8 (see Inset), shows that in the convectively-mixed upper layer the cyclonic eddy has the shape of a truncated cone, the cross-sectional area of which at the base slightly exceeds that on the surface (see vertical sections of *Ro* and *T* in Fig. 9, see Inset). The cyclonic eddy is characterized by very high vertical vorticity in the eddy's center ($\mathrm{Ro} > 2.5$) and pronounced differential rotation (Ro decreases rapidly with increasing distance from the center which is typical for the surface layer cyclonic SCVs [21]. Noticeable that the core of cyclonic eddy in the convectively mixed layer has negative temperature anomaly of approx. 1.5 °C. Negative values of the Richardson number corresponding to the gravitational instability are frequently encountered in the convectively mixed upper layer (see the bottom panels of Fig. 9).

4. Discussion and Conclusions

The results of very high-resolution modelling of the Baltic Sea have shown that the characteristics of submesoscale eddies in summer and winter are substantially different.

In summer, three types of SCVs can be distinguished:

– the surface layer SCVs;
– the cold intermediate layer SCVs;
– the deep haline layer SCVs.

The surface layer SCVs can be both cyclonic and anticyclonic. The most intensive cyclonic SCVs are characterized by fast rotation with maximum value of Ro as large as 2—3, while the minimum value of Ro in the anticyclonic eddies is limited to $\mathrm{Ro} \gtrsim -1$. The surface layer SCVs have the shape of an inverted cone with the base of the cone on the surface; they usually extend vertically up to and including the cold intermediate layer.

The cold intermediate layer SCVs are supported by the seasonal thermocline from above and the permanent halocline from below. They have the shape of concave and convex lenses for cyclones and anticyclones, respectively,

in the density field. Noticeable that the modelling results support the conclusion on dominance of anticyclonic convex lenses over the cyclonic concave lenses in the interior layers of the Baltic Sea (Fig. 6).

The deep haline layer SCVs have smaller lengthscales relative to the cold intermediate layer SCVs, but the shape is identical.

In winter when the seasonal thermocline and cold intermediate layer are replaced by a relatively deep, convectively mixed upper layer, where the convex/anticylonic and concave/cyclonic lenses cannot exist and the cyclonic SCVs dominate. The winter-time cyclonic SCVs have the shape of a truncated cone, the cross-sectional area of which at the base of convectively mixed layer slightly exceeds that on the sea surface. Keeping in mind a remote analogy with the open-ocean deep convection which occurs only in regions of cyclonic circulation [32], we intuitively suppose that the dominance of cyclonic SCVs in the upper mixed layer of the Baltic Sea in winter is somehow linked with gravitational convection caused by cooling from the surface.

Remarkable that the core of winter-time cyclonic eddies is characterized by a negative temperature anomaly throughout the convectively-mixed upper layer. The anomaly is formed because the mixed layer depth is minimum in the cyclonic eddy (Fig. 9) and, therefore, the negative heat flux from the atmosphere is vertically mixed in a thinner layer. It is also important that the rotary circulation of water in the vortex prevents lateral mixing, thereby maintaining the existence of a temperature anomaly.

Successive maps of the simulated vertical vorticity show that a common way to form the SCVs in the Baltic Sea is empirically preceded by a filament or strip of high vertical vorticity. The high-vorticity filament originates above a steep bottom and eventually transforms in a rounded high-vorticity spot, that is a vortex.

Our simulations show that SCVs can live in the Baltic Sea for several months or more. During its life cycle, the SCVs can repeatedly merge with other eddies of the same sign of vorticity, and the merger makes the eddy stronger thereby contributing to its longevity.

5. Acknowledgements and Funding

The allocation of computing time on High Performance Computing cluster by the Tallinn University of Technology and by the University of Tartu is gratefully acknowledged. GETM community in Leibniz Institute of Baltic Sea Research (IOW) is acknowledged for their technical support and the maintenance of model code. Germo Väli was supported by the Estonian Research Council (grant no. PRG602 and grant no. IUT19-6). Victor Zhurbas was supported by the budgetary financing of the Shirshov Institute of Oceanology RAS (Project No. 0128-2021-0001).

Литература

1. *McWilliams J.C.* Submesoscale, coherent vortices in the ocean // Rev. Geophys. 1985. V. 23. P. 165—182. doi: 10.1029/RG023i002p00165
2. *McWilliams J.C.* Vortex generation through balanced adjustment // J. Phys. Oceanogr. 1988. V. 18. P. 1178—1192. doi: 10.1175/1520—0485(1988)018<1178: VGTBA>2.0.CO;2
3. *Armi L.*, *Hebert D.*, *Oakey N.*, *Price J.F.*, *Richardson P.L.*, *Rossby H.T.*, *Rudduck B.* Two years in the life of a Mediterraneam salt lens // J. Phys. Oceanogr. 1989. V. 19. P. 354—370. doi: 10.1175/1520—0485(1989)019<0354: TYITLO>2.0.CO;2
4. *Бенилов А.Ю., Саффрай А.С., Филюшкин Б.Н., Кожелупова Н.Г.* О нелинейной динамике линз средиземноморской воды «медди» // Фундам. прикл. гидрофиз. 2020. Т. 13, № 3. С. 20—42. doi: 10.7868/S2073667320030028
5. *McWilliams J.*C. Submesoscale currents in the ocean // Proc. R. Soc. A. 2016. V. 472. 20160117. doi: 10.1098/rspa.2016.0117
6. *Журбас В.М., Кузьмина Н.П.* О растекании перемешанного пятна во вращающейся устойчиво стратифицированной жидкости // Изв. АН СССР, сер. ФАО. 1981. Т. 17, № 3. С. 286—295.
7. *D'Asaro E.* Generation of submesoscale vortices: a new mechanism // J. Geophys. Res. 1988. V. 93. P. 6685—6693. doi: 10.1029/JC093iC06p06685
8. *Gula J.*, *Molemaker M.J.*, *McWilliams J.C.* Gulf Stream dynamics along the southeastern U. S. Seaboard // J. Phys. Oceanogr. 2015. V. 45. P. 690—715. doi: 10.1175/JPO-D-14-0154.1
9. *Elken J., Pajuste M., Kõuts T.* On intrusive lenses and their role in mixing in the Baltic deep layers // Proceedings of the Conference of the Baltic Oceanographers, Kiel. 1988. 1. P. 367—376.
10. *Zhurbas V.M.*, *Paka V.T.* Mesoscale thermohaline variability in the Eastern Gotland Basin following the 1993 major Baltic inflow // J. Geophys. Res. 1997. V. 102(C9). P. 20917—20926. doi: 10.1029/97JC00443
11. *Sellschopp J.*, *Arneborg L.*, *Knoll M.*, *Fiekas V.*, *Gerdes F.*, *Burchard H.*, *Lass H.U.*, *Mohrholz V.*, *Umlauf L.* Direct observations of medium-intensity inflow into the Baltic Sea // Cont. Shelf Res. 2006. V. 26. P. 2393—2414. doi: 10.1016/j.csr.2006.07.004

12. *Piechura J.*, *Beszczyńska-Möller A.* Inflow waters in the deep regions of the Southern Baltic Sea – transport and transformations // Oceanologia. 2003. V. 45(4). P. 593—621.

13. *Zhurbas V., Stipa T., Mälkki P., Paka V., Golenko N., Hense I., Sklyarov V.* Generation of subsurface cyclonic eddies in the southeast Baltic Sea: observations and numerical experiments // J. Geophys. Res. Oceans. 2004. 109. C05033. doi: 10.1029/2003JC002074

14. *Zhurbas V.M., Oh I.S., Paka V.T.* Generation of cyclonic eddies in the Eastern Gotland Basin of the Baltic Sea following dense water inflows: numerical experiments // J. Mar. Sys. 2003. V. 38. P. 323—336. doi: 10.1016/S0924-7963(02)00251-8

15. *Zhurbas V., Elken J., Paka V., Piechura J., Väli G., Chubarenko I., Golenko N., Shchuka S.* Structure of unsteady overflow in the Słupsk Furrow of the Baltic Sea // J. Geophys. Res. Oceans. 2012. V. 117. C04027. doi: 10.1029/2011JC007284

16. *Spall M.A., Price J.F.* Mesoscale variability in the Denmark Strait: the PV outflow hypothesis // J. Phys. Oceanogr. 1998. V. 28. P. 1598—1623. doi: 10.1175/1520-0485(1998)028<1598: MVIDST>2.0.CO;2

17. *Каримова С.С., Лаврова О.Ю., Соловьев Д.М.* Наблюдение вихревых структур в Балтийском море с использованием радиолокационных и радиометрических данных // Исследование Земли из космоса. 2011. № 5. С. 15—23. doi: 10.1134/S0001433812090071

18. *Laanemets J.*, *Väli G.*, *Zhurbas V.*, *Elken J.*, *Lips I.*, *Lips U.* Simulation of mesoscale structures and nutrient transport during summer upwelling events in the Gulf of Finland in 2006 // Boreal Environ. Res. 2011. V. 16(A). P. 15—26.

19. *Väli G.*, *Zhurbas V.*, *Lips U.*, *Laanemets J.* Submesoscale structures related to upwelling events in the Gulf of Finland, Baltic Sea (numerical experiments) // J. Mar. Syst. 2017. 171(SI). P. 31—42. doi: 10.1016/j.jmarsys.2016.06.010

20. *Вяли Г., Журбас В., Липс У., Лаанеметс Я.* Кластеризация плавающих частиц из-за субмезомасштабной динамики: модельное исследование для Финского залива Балтийского моря // Фундам. прикл. гидрофиз. 2018. Т. 11, № 2. С. 21—35. doi: 10.7868/S2073667318020028

21. *Zhurbas V., Väli G., Kuzmina N.* Rotation of floating particles in submesoscale cyclonic and anticyclonic eddies: a model study for the southeastern Baltic Sea // Ocean Sci. 2019. 15. P. 1691—1705. doi: 10.5194/os-15-1691-2019

22. *Reißmann J.H.* An algorithm to detect isolated anomalies in three-dimensional stratified data fields with an application to density fields from four deep basins of the Baltic Sea // J. Geophys. Res. 2005. V. 110. C12018. doi: 10.1029/2005JC002885

23. *Vortmeyer-Kley R., Holtermann P.L., Feudel U., Gräwe U.* Comparing Eulerian and Lagrangian eddy census for a tideless, semi-enclosed basin, the Baltic Sea // Ocean Dyn. 2019. V. 69. P. 701—717. doi: 10.1007/s10236-019-01269-z

24. *Burchard H.*, *Bolding K.* GETM – a general estuarine transport model, Scientific documentation, Technical report EUR20253 en. // Tech. rep., European Commission. Ispra, Italy, 2002.

25. *Hofmeister R.*, *Burchard H.*, *Beckers J-M.* Non-uniform adaptive vertical grids for 3D numerical ocean models // Ocean Model. 2010. V. 33(1—2). P. 70—86. doi: 10.1016/j.ocemod.2009.12.003

26. *Gräwe U.*, *Holtermann P.*, *Klingbeil K.*, *Burchard H.* Advantages of vertically adaptive coordinates in numerical models of stratified shelf seas // Ocean Model. 2015. V. 92. P. 56—68. doi: 10.1016/j.ocemod.2015.05.008

27. *Burchard H.*, *Bolding K.* Comparative Analysis of Four Second-Moment Turbulence Closure Models for the Oceanic Mixed Layer // J. Phys. Oceanogr. 2001. V. 31. P. 1943—1968. doi: 10.1175/1520-0485(2001)031<1943: CAOFSM>2.0.CO;2

28. *Canuto V.M.*, *Howard A.*, *Cheng Y.*, *Dubovikov M.S.* Ocean Turbulence. Part I: One-Point Closure Model – Momentum and Heat Vertical Diffusivities // J. Phys. Oceanogr. 2001. V. 31. P. 1413—1426. doi: 10.1175/1520-0485(2001)031<1413: OTPIOP>2.0.CO;2

29. *Zhurbas V., Väli G., Golenko M., Paka V.* Variability of bottom friction velocity along the inflow water pathway in the Baltic Sea // J. Mar. Syst. 2018. V. 184. P. 50—58. doi: 10.1016/j.jmarsys.2018.04.008

30. *Liblik T., Väli G., Lips I., Lilover M.-J., Kikas V., Laanemets J.* The winter stratification phenomenon and its consequences in the Gulf of Finland, Baltic Sea // Ocean Sci. 2020. V. 16. P. 1475—1490. doi: 10.5194/os-16-1475-2020

31. *Männik A.*, *Merilain M.* Verification of different precipitation forecasts during extended winter-season in Estonia // HIRLAM Newsletter. 2007. 52. P. 65—70.

32. *Killworth P.D.* Deep convection in the World Ocean // Rev. Geophys. 1983. 21. P. 1—26. doi: 10.1029/RG021i001p00001

References

1. *McWilliams J.C.* Submesoscale, coherent vortices in the ocean. *Rev. Geophys.* 1985, 23, 165—182. doi: 10.1029/RG023i002p00165

2. *McWilliams J.*C. Vortex generation through balanced adjustment. *J. Phys. Oceanogr.* 1988, 18, 1178—1192. doi: 10.1175/1520-0485(1988)018<1178: VGTBA>2.0.CO;2

3. *Armi L.*, *Hebert D.*, *Oakey N.*, *Price J. F.*, *Richardson P. L.*, *Rossby H. T.*, *Rudduck B.* Two years in the life of a Mediterraneam salt lens. *J. Phys. Oceanogr.* 1989, 19, 354—370. doi: 10.1175/1520-0485(1989)019<0354: TYITLO>2.0.CO;2

4. *Benilov A.Yu., Safray A.S., Filyushkin B.N., Kojelupova N.G.* On nonlinear dynamics of Meddies. *Fundam. Prikl. Gidrofiz.* 2020, 13, 3, 20—42 (in Russian). doi: 10.7868/S2073667320030028
5. *McWilliams J.*C. Submesoscale currents in the ocean. *Proc. R. Soc. A.* 2016, 72, 20160117. doi: 10.1098/rspa.2016.0117
6. *Zhurbas V.M., Kuzmina N.P.* On the spreading of a mixed patch in a rotating stably stratified fluid. *Izv. Acad. Sci. SSSR, Atmos. and Oceanic Phys.* 1981, 17(3), 211—217.
7. *D'Asaro E.* Generation of submesoscale vortices: a new mechanism. *J. Geophys. Res.* 1988, 93, 6685—6693. doi: 10.1029/JC093iC06p06685
8. *Gula J.*, *Molemaker M.J.*, *McWilliams J.C.* Gulf Stream dynamics along the southeastern U. S. Seaboard. *J. Phys. Oceanogr.* 2015, 45, 690—715. doi: 10.1175/JPO-D-14-0154.1
9. *Elken J., Pajuste M., Kõuts T.* On intrusive lenses and their role in mixing in the Baltic deep layers. *Proceedings of the Conference of the Baltic Oceanographers, Kiel.* 1988, 1, 367—376.
10. *Zhurbas V.M., Paka V.T.* Mesoscale thermohaline variability in the Eastern Gotland Basin following the 1993 major Baltic inflow. *J. Geophys. Res.* 1997, 102(C9), 20917—20926. doi: 10.1029/97JC00443
11. *Sellschopp J.*, *Arneborg L.*, *Knoll M.*, *Fiekas V.*, *Gerdes F.*, *Burchard H.*, *Lass H.U.*, *Mohrholz V.*, *Umlauf L.* Direct observations of medium-intensity inflow into the Baltic Sea. *Cont. Shelf Res.* 2006, 26, 2393—2414. doi: 10.1016/j.csr.2006.07.004
12. *Piechura J.*, *Beszczyńska-Möller A.* Inflow waters in the deep regions of the Southern Baltic Sea – transport and transformations. *Oceanologia*. 2003, 45(4), 593—621.
13. *Zhurbas V., Stipa T., Mälkki P., Paka V., Golenko N., Hense I., Sklyarov V.* Generation of subsurface cyclonic eddies in the southeast Baltic Sea: observations and numerical experiments. *J. Geophys. Res. Oceans*. 2004, 109, C05033. doi: 10.1029/2003JC002074
14. *Zhurbas V.M.*, *Oh I.S.*, *Paka V.T.* Generation of cyclonic eddies in the Eastern Gotland Basin of the Baltic Sea following dense water inflows: Numerical experiments. *J. Mar. Sys*. 2003, 38, 323—336. doi: 10.1016/S0924-7963(02)00251-8
15. *Zhurbas V., Elken J., Paka V., Piechura J., Väli G., Chubarenko I., Golenko N., Shchuka S.* Structure of unsteady overflow in the Słupsk Furrow of the Baltic Sea. *J. Geophys. Res. Oceans*. 2012, 117, C04027. doi: 10.1029/2011JC007284
16. *Spall M.A., Price J.F.* Mesoscale variability in the Denmark Strait: the PV outflow hypothesis. *J. Phys. Oceanogr.* 1998, 28, 1598—1623. doi: 10.1175/1520-0485(1998)028<1598: MVIDST>2.0.CO;2
17. *Karimova S.S., Lavrova O.Yu., Solov'ev D.M.* Observation of eddy structures in the Baltic Sea with the use of radiolocation and radiometric satellite data. *Izv. Atm. Ocean. Phys.* 2012, 48(9), 1006—1013. doi: 10.1134/S0001433812090071
18. *Laanemets J.*, *Väli G.*, *Zhurbas V.*, *Elken J.*, *Lips I.*, *Lips U.* Simulation of mesoscale structures and nutrient transport during summer upwelling events in the Gulf of Finland in 2006. *Boreal Environ. Res.* 2011, 16(A), 15—26.
19. *Väli G.*, *Zhurbas V.*, *Lips U., Laanemets J.* Submesoscale structures related to upwelling events in the Gulf of Finland, Baltic Sea (numerical experiments). *J. Mar. Syst.* 2017, 171(SI), 31—42. doi: 10.1016/j.jmarsys.2016.06.010
20. *Väli G.*, *Zhurbas V.*, *Lips U.*, *Laanemets J.* Clustering of floating particles due to submesoscale dynamics: a simulation study for the Gulf of Finland, Baltic Sea. *Fudam. Prikl. Gidrofiz.* 2018, 11 (2), 21—35. doi: 10.7868/S2073667318020028
21. *Zhurbas V., Väli G., Kuzmina N.* Rotation of floating particles in submesoscale cyclonic and anticyclonic eddies: a model study for the southeastern Baltic Sea. *Ocean Sci*. 2019, 15, 1691—1705. doi: 10.5194/os-15-1691-2019
22. *Reißmann J.H.* An algorithm to detect isolated anomalies in three-dimensional stratified data fields with an application to density fields from four deep basins of the Baltic Sea. *J. Geophys. Res.* 2005, 110, C12018. doi: 10.1029/2005JC002885
23. *Vortmeyer-Kley R.*, *Holtermann P.L.*, *Feudel U.*, *Gräwe U.* Comparing Eulerian and Lagrangian eddy census for a tide-less, semi-enclosed basin, the Baltic Sea. *Ocean Dyn*. 2019, 69, 701—717. doi: 10.1007/s10236-019-01269-z
24. *Burchard H.*, *Bolding K.* GETM – a general estuarine transport model, Scientific documentation, Technical report EUR20253 en. *Tech. rep.*, *European Commission. Ispra*, *Italy*, 2002.
25. *Hofmeister R.*, *Burchard H.*, *Beckers J-M.* Non-uniform adaptive vertical grids for 3D numerical ocean models. *Ocean Model.* 2010, 33(1—2), 70—86. doi: 10.1016/j.ocemod.2009.12.003
26. *Gräwe U.*, *Holtermann P.*, *Klingbeil K.*, *Burchard H.* Advantages of vertically adaptive coordinates in numerical models of stratified shelf seas. *Ocean Model.* 2015, 92, 56—68, doi: 10.1016/j.ocemod.2015.05.008
27. *Burchard H.*, *Bolding K.* Comparative Analysis of Four Second-Moment Turbulence Closure Models for the Oceanic Mixed Layer. *J. Phys. Oceanogr.* 2001, 31, 1943—1968. doi: 10.1175/1520-0485(2001)031<1943: CAOFSM>2.0.CO;2
28. *Canuto V.M.*, *Howard A.*, *Cheng Y.*, *Dubovikov M.S.* Ocean Turbulence. Part I: One-Point Closure Model – Momentum and Heat Vertical Diffusivities. *J. Phys. Oceanogr.* 2001, 31, 1413—1426. doi: 10.1175/1520-0485(2001)031<1413: OTPIOP>2.0.CO;2
29. *Zhurbas V., Väli G., Golenko M., Paka V.* Variability of bottom friction velocity along the inflow water pathway in the Baltic Sea. *J. Mar. Syst.* 2018, 184, 50—58. doi: 10.1016/j.jmarsys.2018.04.008

30. *Liblik T., Väli G., Lips I., Lilover M.-J., Kikas V., Laanemets J.* The winter stratification phenomenon and its consequences in the Gulf of Finland, Baltic Sea. *Ocean Sci*. 2020, 16, 1475—1490. doi: 10.5194/os-16-1475-2020

31. *Männik A.*, *Merilain M.* Verification of different precipitation forecasts during extended winter-season in Estonia. *HIRLAM Newsletter*. 2007, 52, 65—70.

32. *Killworth P.D.* Deep convection in the World Ocean. *Rev. Geophys.* 1983, 21, 1—26. doi: 10.1029/RG021i001p00001

К статье *Вяли Г., Журбас В.М.* Сезонность субмезомасштабных когерентных вихрей в северной Балтике: модельное исследование

Väli G., Zhurbas V.M. Seasonality of submesoscale coherent vortices in the Northern Baltic Proper: a model study

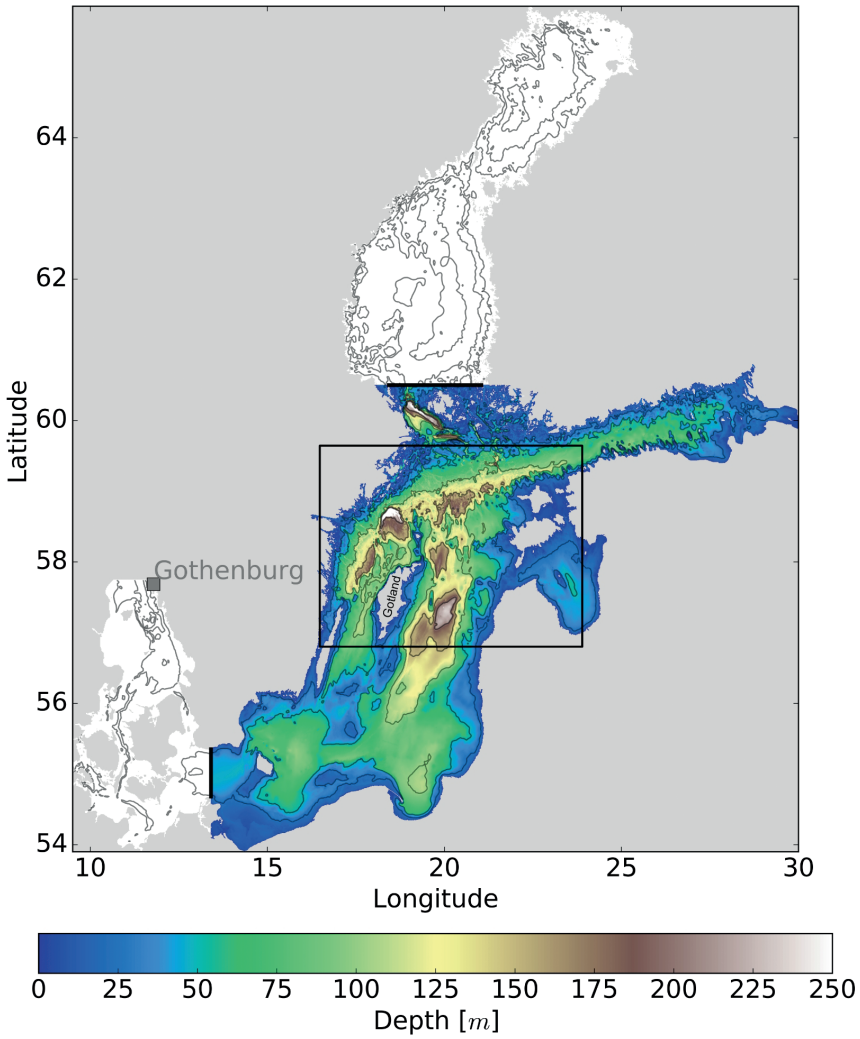

Fig. 1. Bathymetric map of the Baltic Sea. The very high-resolution model domain (filled colors) with the open boundary locations (black bold lines). The coarse resolution model domain (blank contours + filled colors) has an open boundary close to the Gothenburg. The study area is within the rectangle.

К статье *Вяли Г., Журбас В.М.* Сезонность субмезомасштабных когерентных вихрей в северной Балтике: модельное исследование

Väli G., Zhurbas V.M. Seasonality of submesoscale coherent vortices in the Northern Baltic Proper: a model study

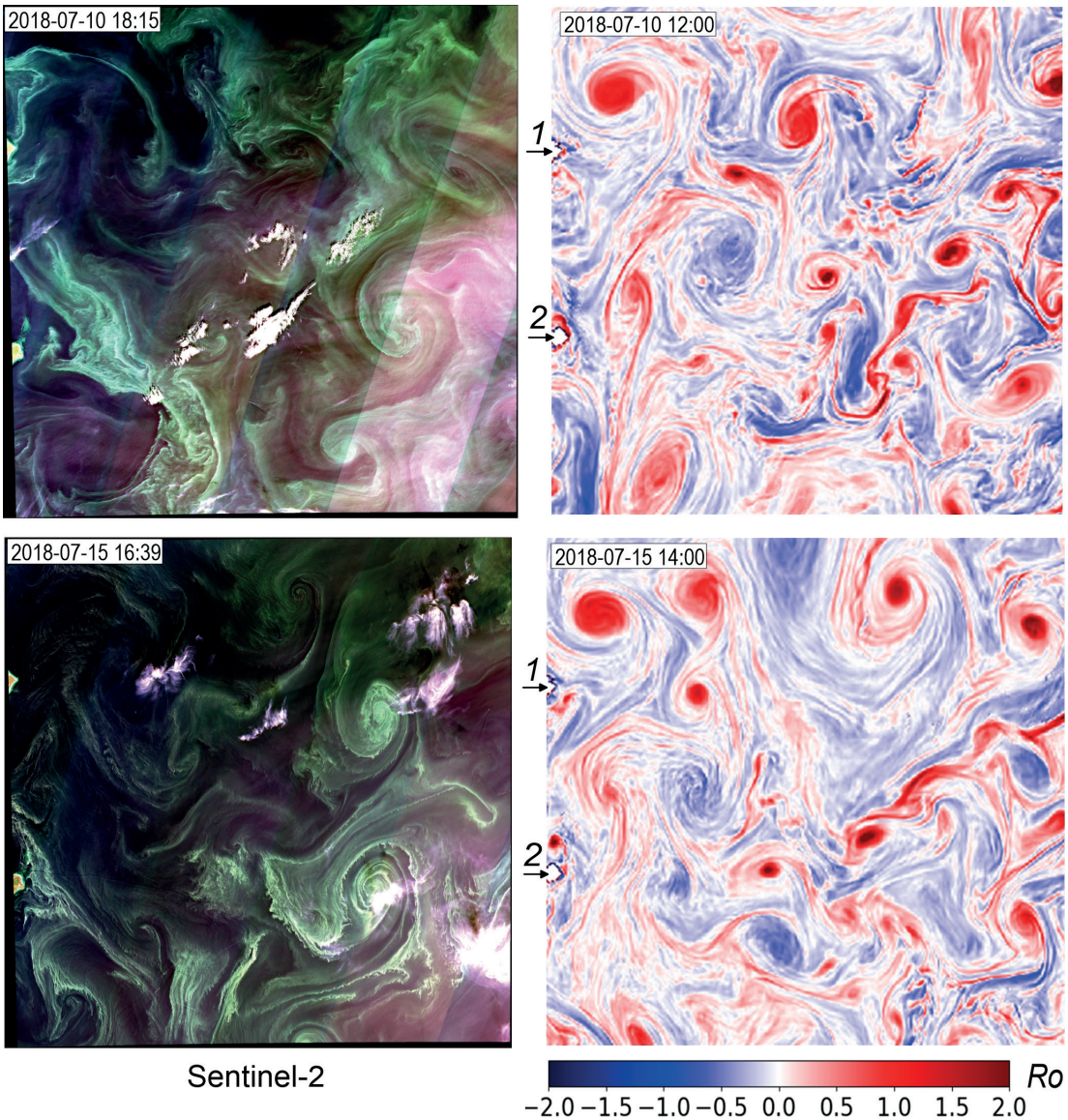

Fig. 2. Snapshots of a 1°× 1°=111 km × 111 km area of the northern Baltic Proper to the northeast of the Gotland Island dated 2018-07-10 (top panels) and 2018-07-15 (bottom panels). The left panels are the optical remote sensing images from Sentinel-2. The right panels are the maps of the Rossby number in the surface layer simulated by the very high-resolution model. The arrows labelled 1 and 2 point at the eastern tips of the Swedish islands of Gotska Sandön and Fårö, respectively. The remote sensing images were downloaded from https://eos.com/landviewer (last access: 21 June 2021),

К статье *Вяли Г., Журбас В.М.* Сезонность субмезомасштабных когерентных вихрей в северной Балтике: модельное исследование

Väli G., Zhurbas V.M. Seasonality of submesoscale coherent vortices in the Northern Baltic Proper: a model study

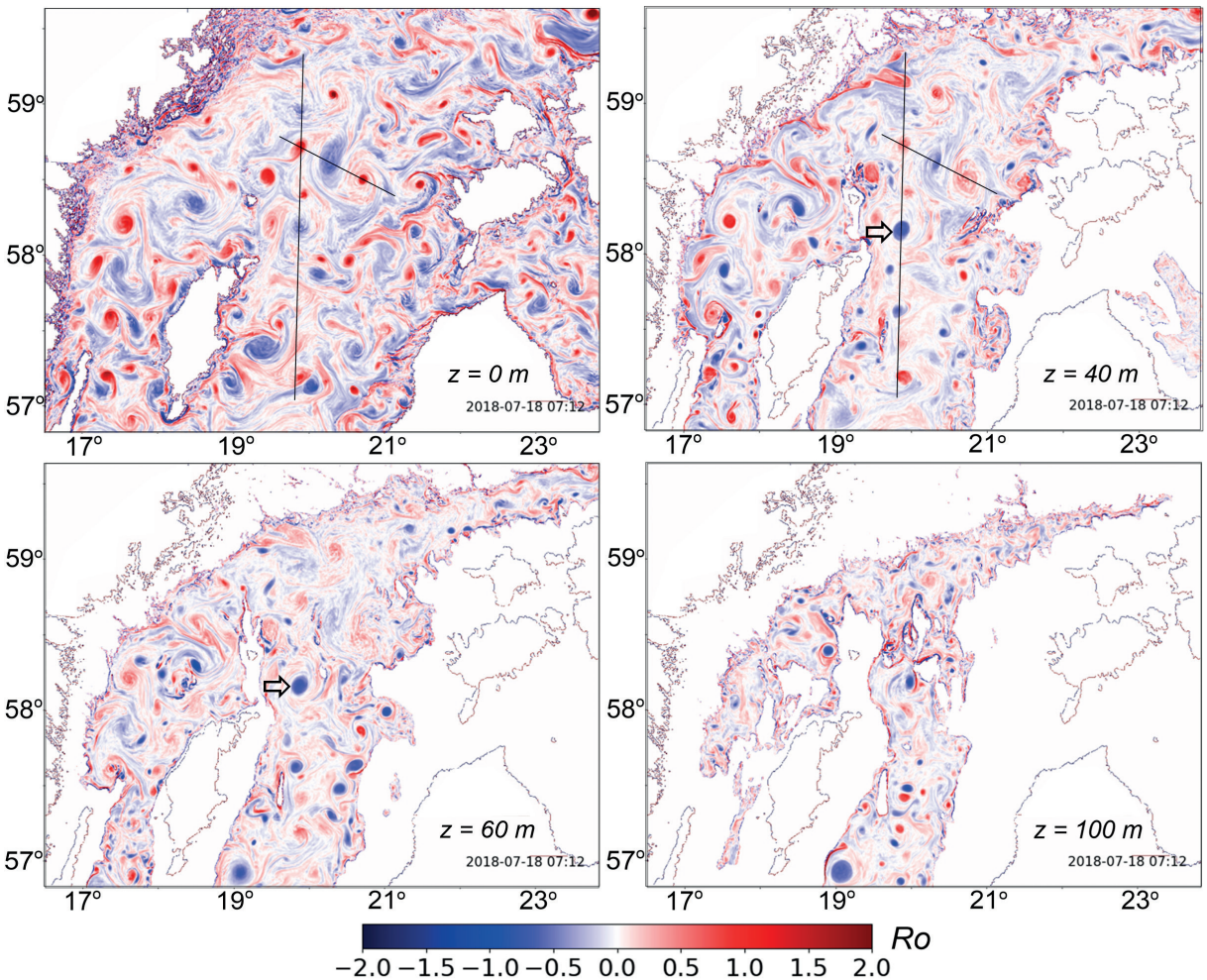

Fig. 3. Maps of the gradient Rossby number Ro at z-levels of 0, 40, 60, and 100 m (simulation on 2018-07-18 07:12 GMT illustrating the summertime case). The intersecting straight line segments show the vertical sections presented in Fig. 4. The arrow points at a subsurface anticyclonic lens that can be identified in the following Figs. 4 and 6.

К статье *Вяли Г., Журбас В.М.* Сезонность субмезомасштабных когерентных вихрей в северной Балтике: модельное исследование

Väli G., Zhurbas V.M. Seasonality of submesoscale coherent vortices in the Northern Baltic Proper: a model study

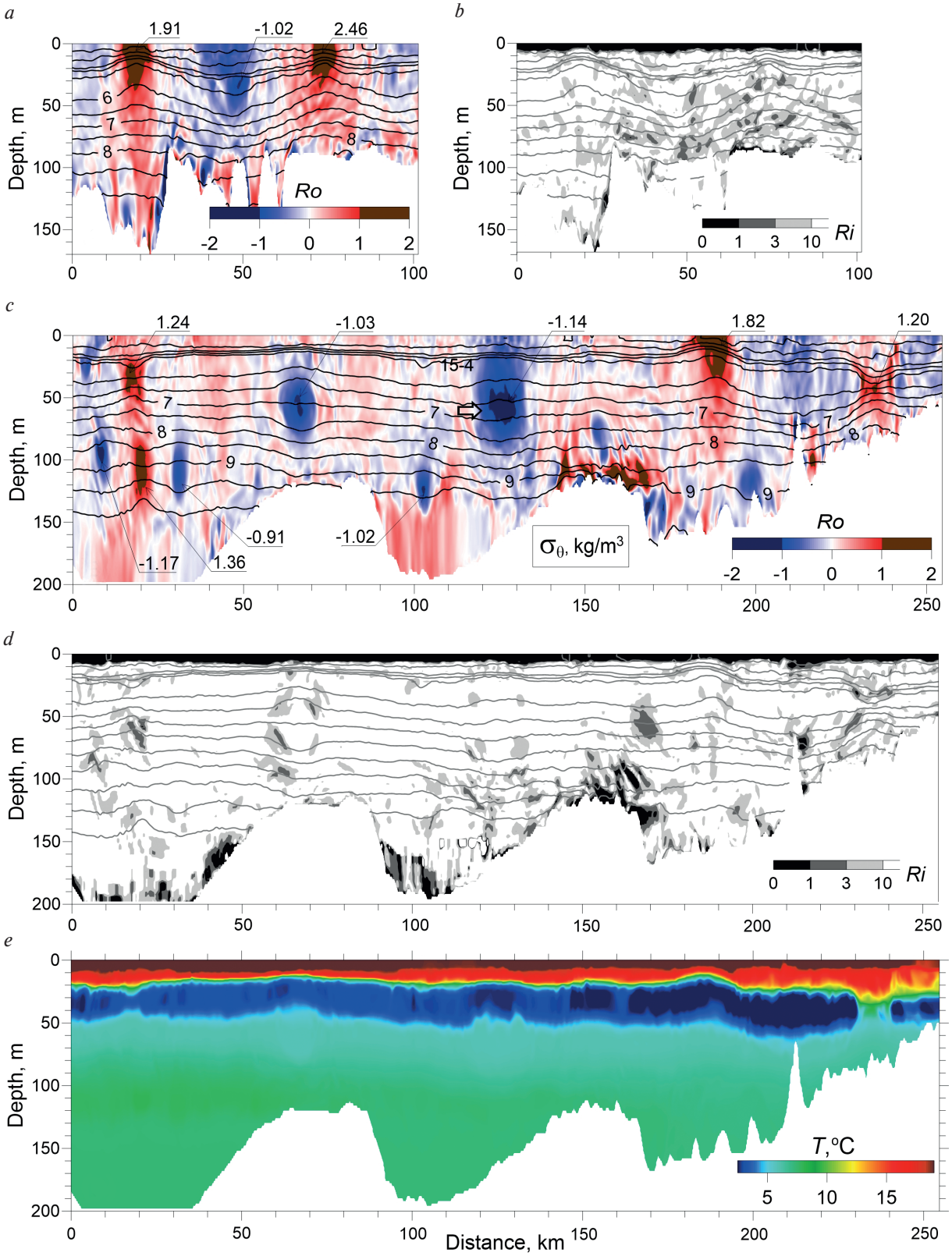

Fig. 4. Rossby number Ro (*a*, *c*), Richardson number Ri (*b*, *d*) and potential density anomaly σ_θ (contours) versus distance and depth for two sections shown in Fig. 3, as well as temperature for the longer section (*e*). Numbers above and below the Ro panels are the extreme values of Ro in the SCVs.

К статье *Вяли Г., Журбас В.М.* Сезонность субмезомасштабных когерентных вихрей в северной Балтике: модельное исследование

Väli G., Zhurbas V.M. Seasonality of submesoscale coherent vortices in the Northern Baltic Proper: a model study

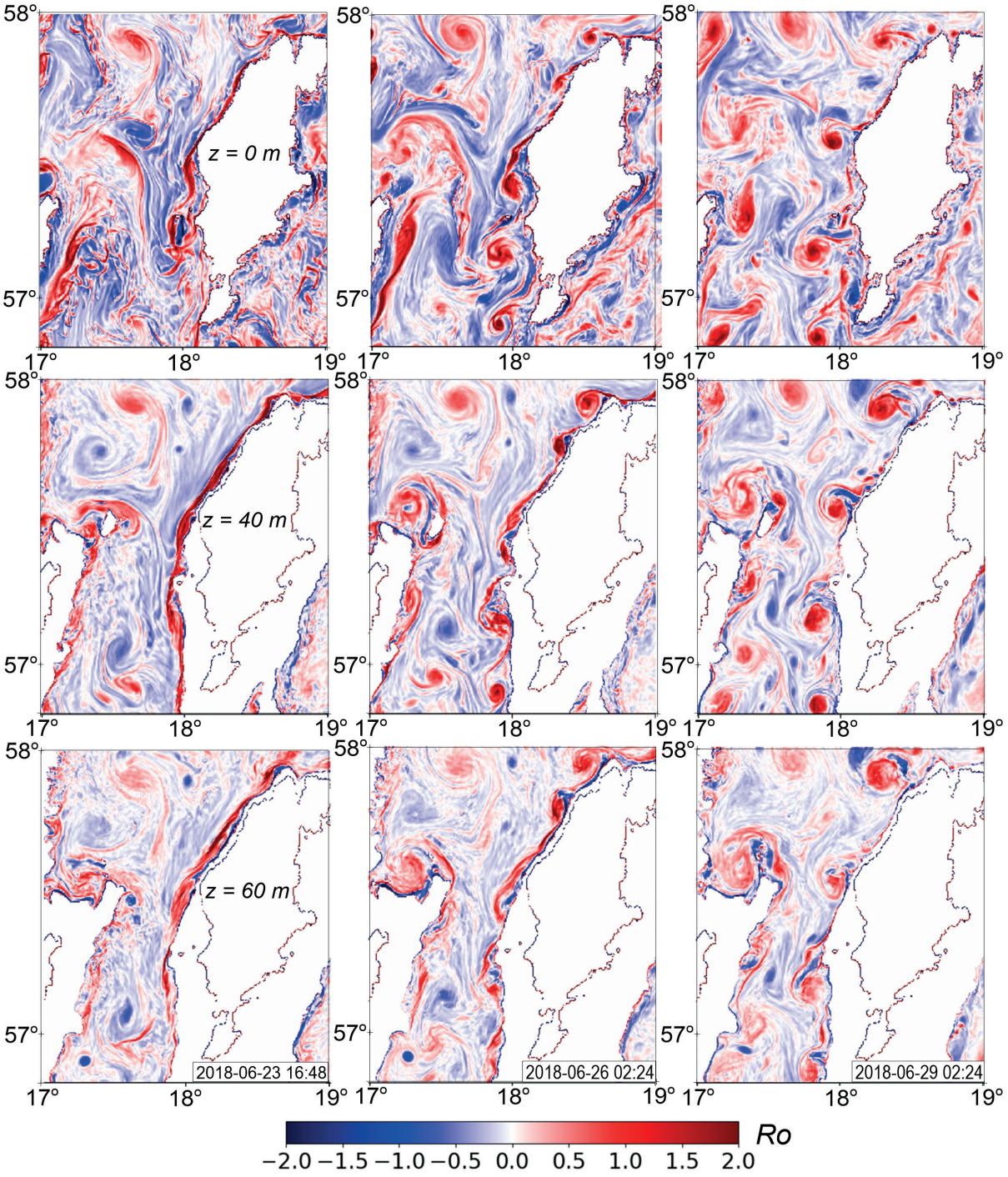

Fig. 5. Snapshots of the Ro maps at different z-levels and time illustrating the formation of a chain of submesoscale cyclonic eddies along the western coast of the Gotland Island.

К статье *Вяли Г., Журбас В.М.* Сезонность субмезомасштабных когерентных вихрей в северной Балтике: модельное исследование

Väli G., Zhurbas V.M. Seasonality of submesoscale coherent vortices in the Northern Baltic Proper: a model study

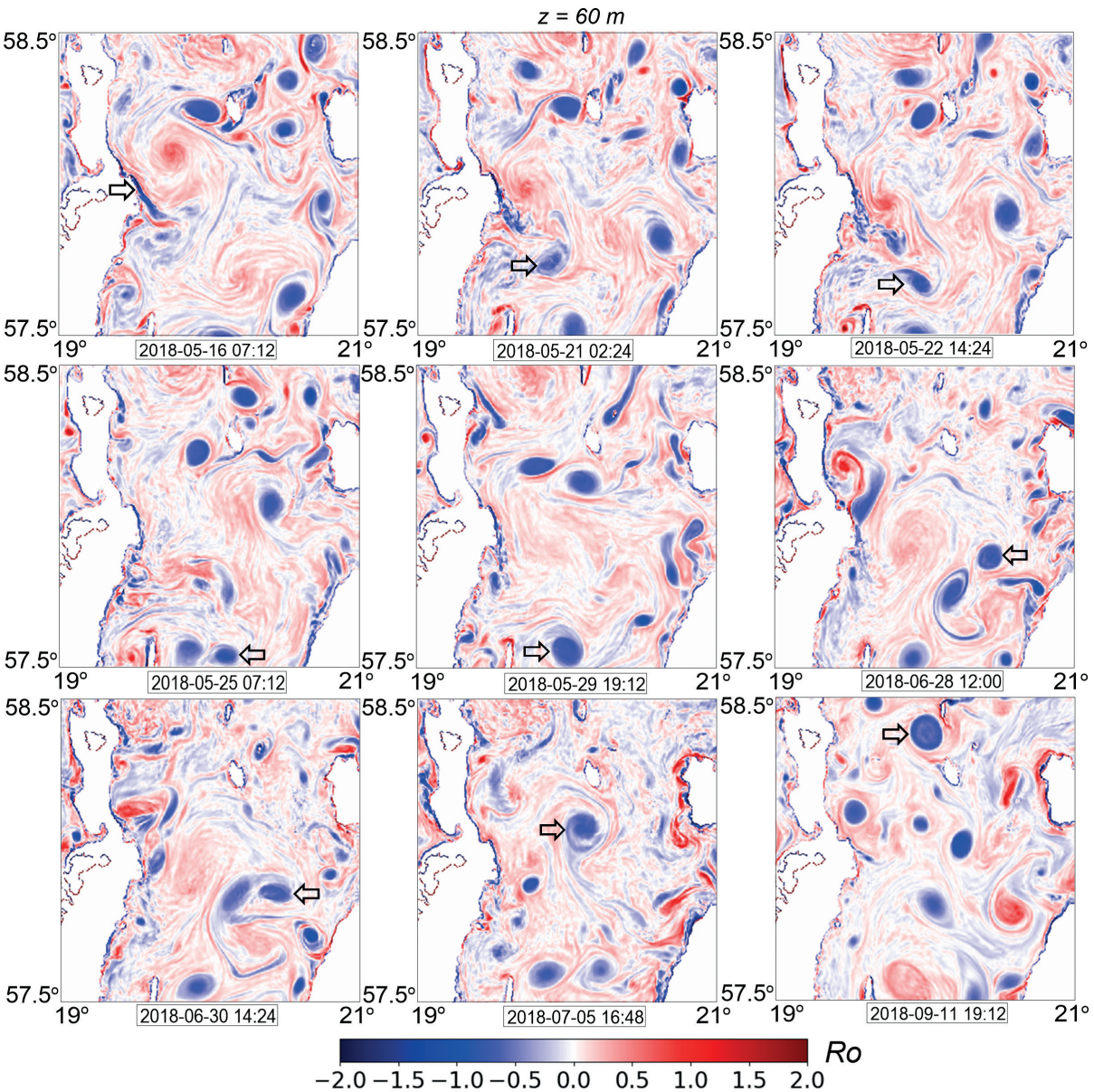

Fig. 6. Snapshots of the Ro maps at 60 m z-level and different time illustrating the formation and life cycle of a subsurface anticyclonic lens pointed by the arrow.

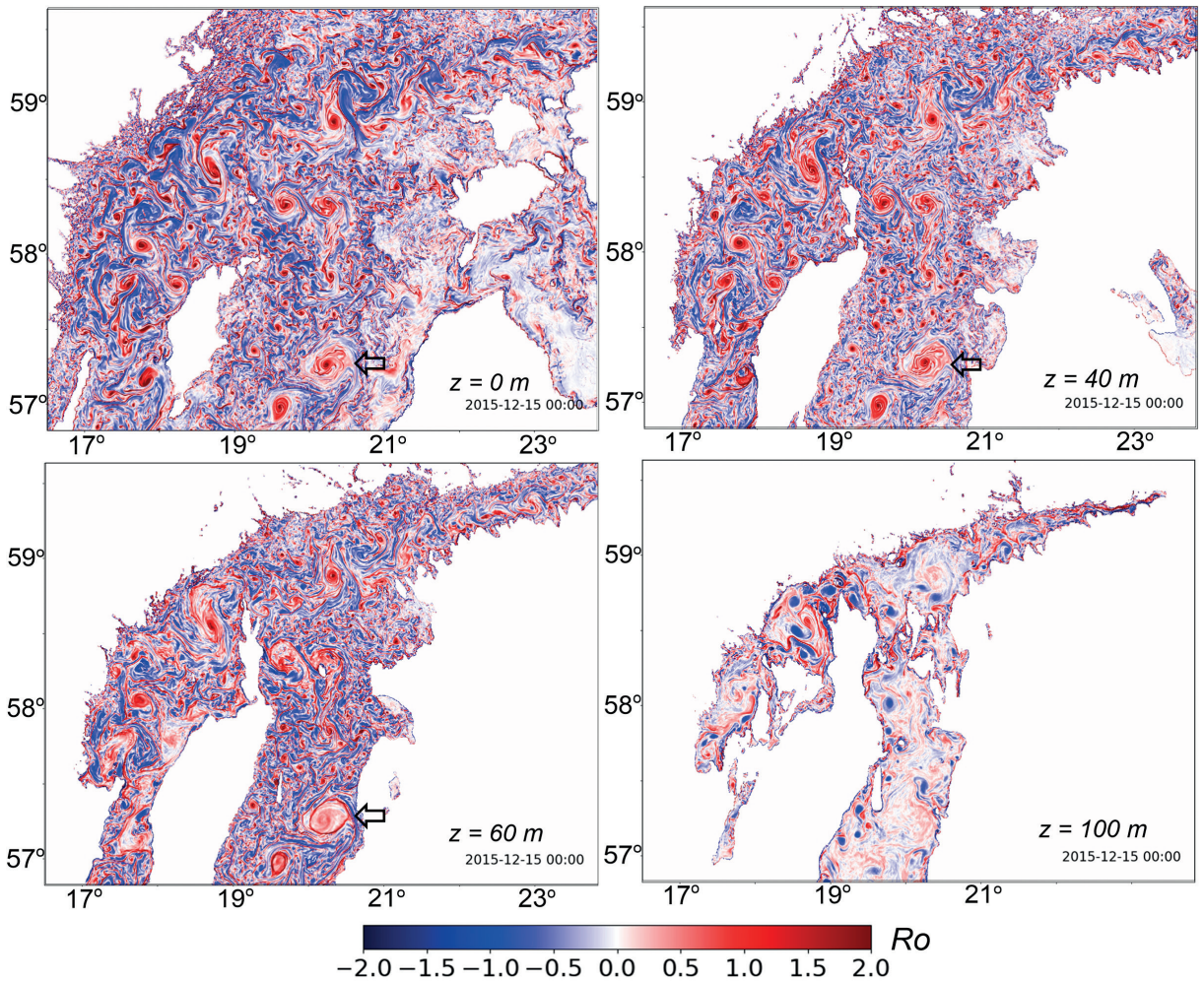

Fig. 7. Maps of Ro at z-levels of 0, 40, 60, and 100 m (simulation on 2015-12-15 00:00 GMT illustrating the wintertime case). The arrow points at a cyclonic SCV the side view of which is presented in Fig. 9 (see also Fig. 8).

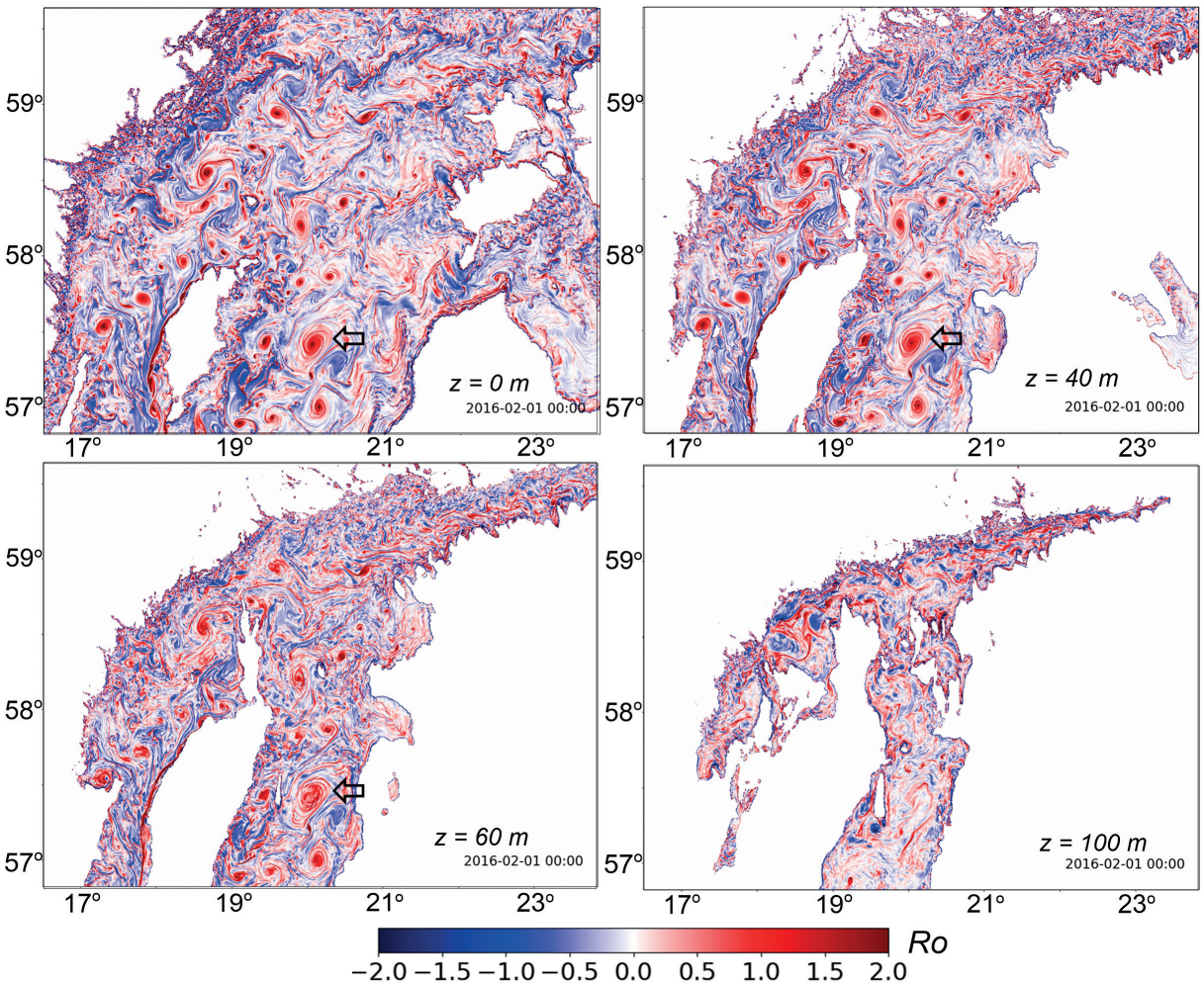

Fig. 8. Maps of Ro at z-levels of 0, 40, 60, and 100 m (simulation on 2016-02-01 00:00 GMT) illustrating the wintertime case. The arrow points at a cyclonic SCV the side view of which is presented in Fig. 9 (see also Fig. 7).

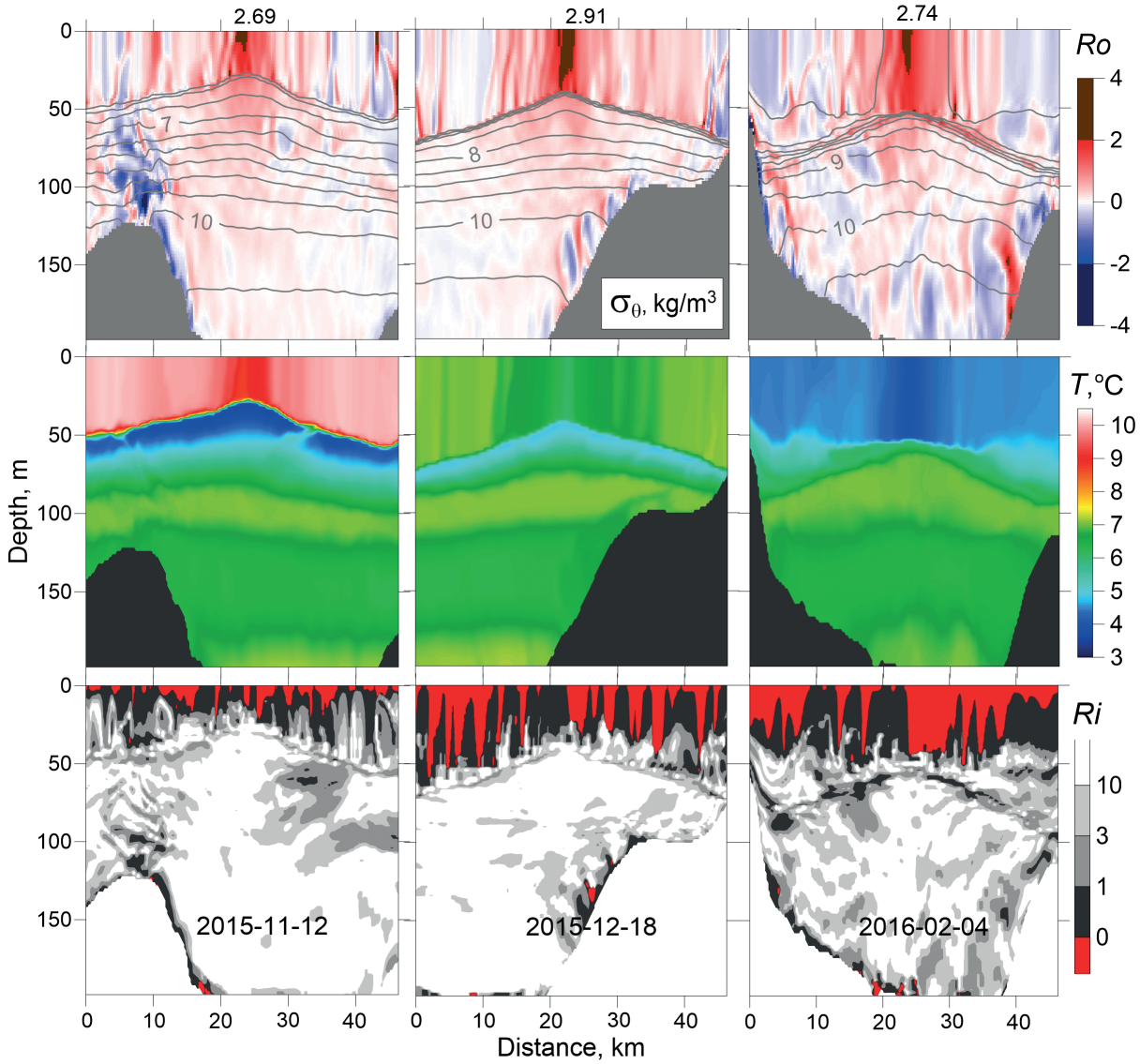

Fig. 9. Rossby number Ro, Richardson number Ri, temperature T and potential density anomaly σ_θ versus distance and depth for a zonal section across the center of the cyclonic SCV pointed by the arrow in Figs. 7 and 8.